

# Confined Crystals of the Smallest Phase-Change Material

Cristina E. Giusca,<sup>\*,†,‡</sup> Vlad Stolojan,<sup>†</sup> Jeremy Sloan,<sup>‡</sup> Felix Börrnert,<sup>§,∇</sup> Hidetsugu Shiozawa,<sup>†,○</sup> Kasim Sader,<sup>||</sup> Mark H. Rummeli,<sup>§,⊥</sup> Bernd Büchner,<sup>§</sup> and S. Ravi P. Silva<sup>†</sup>

<sup>†</sup>Advanced Technology Institute, University of Surrey, Guildford, GU2 7XH, United Kingdom

<sup>‡</sup>Department of Physics, University of Warwick, Coventry, CV4 7AL, United Kingdom

<sup>§</sup>IFW Dresden, P.O. Box 270116, Dresden, D-01171, Germany

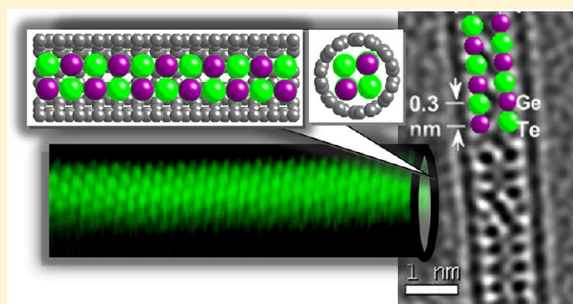
<sup>||</sup>UK SuperSTEM, Daresbury Laboratory, Warrington, WA4 4AD, United Kingdom

<sup>⊥</sup>Technische Universität Dresden, D-01062, Dresden, Germany

## Supporting Information

**ABSTRACT:** The demand for high-density memory in tandem with limitations imposed by the minimum feature size of current storage devices has created a need for new materials that can store information in smaller volumes than currently possible. Successfully employed in commercial optical data storage products, phase-change materials, that can reversibly and rapidly change from an amorphous phase to a crystalline phase when subject to heating or cooling have been identified for the development of the next generation electronic memories. There are limitations to the miniaturization of these devices due to current synthesis and theoretical considerations that place a lower limit of 2 nm on the minimum bit size, below which the material does not transform in the structural phase. We show here that by using carbon nanotubes of less than 2 nm diameter as templates phase-change nanowires confined to their smallest conceivable scale are obtained. Contrary to previous experimental evidence and theoretical expectations, the nanowires are found to crystallize at this scale and display amorphous-to-crystalline phase changes, fulfilling an important prerequisite of a memory element. We show evidence for the smallest phase-change material, extending thus the size limit to explore phase-change memory devices at extreme scales.

**KEYWORDS:** Phase-change materials, GeTe, carbon nanotubes, scanning tunneling microscopy, electron microscopy



Repeated and reversible switching of phase-change materials, generally chalcogenide alloys, between the crystalline and the amorphous phase is used in commercial data storage products, such as compact disks (CDs), digital versatile disks (DVDs), and Blu-ray disks, based on their pronounced optical reflectivity contrast of the two structurally distinct phases.<sup>1–4</sup> Most recently, these materials have been identified for developing the next generation Phase Change Random Access Memory or PCRAM by academia and industry but were considered to have reached a minimum thickness size (i.e., for thin films) of 2 nm.<sup>3,5,6,8,19,20</sup> The PCRAM relies on reversibly driving the phase-change compound between a highly resistive amorphous state corresponding to ones (or ON state) and a conductive crystalline state corresponding to zeros (or OFF state) via electric-field induced Joule heating.<sup>4–7</sup>

We report here on the controlled fabrication of the thinnest phase-change material, possibly suitable for implementation in a matrix-addressed storage structure.<sup>9</sup> By exploiting the unique dimensions and the geometry of nanometer-diameter single-walled carbon nanotubes (SWNTs), an ingenious design for phase-change memory using carbon nanotube electrodes for switching has recently been demonstrated with a drastic reduction in operational power.<sup>10</sup> Also involving phase change nanowires and carbon nanotube electrodes, a memory device

has been fabricated that shows very low programming currents and outstanding electrical characteristics.<sup>11</sup>

Numerous phase-change materials have been developed previously with dimensionality ranging from thin films<sup>12–14</sup> to nanoparticles<sup>15</sup> and to nanowires.<sup>16–18</sup> As dimensions reduce, fundamental physical properties that render these materials suitable for nonvolatile memory applications, such as crystallization speed, melting temperature, thermal stability, electrical resistivity, and threshold voltage change. Previous studies have successfully validated favorable changes of relevant parameters with down-scaling,<sup>5,6,16</sup> however thermodynamic considerations limit the minimum bit size to 2 nm,<sup>5,6,19</sup> under which these materials do not display a change in the structural phase. Moreover, upper limits to the crystallization of thin films of 2 nm thickness have been reported experimentally.<sup>3,8,20</sup> Although phase-change nanowires have been proposed as viable alternatives to thin film counterparts, the diameters of the nanowires synthesized via a vapor–liquid–solid growth range between 200 and 20 nm, depending on the size of the catalyst

**Received:** March 21, 2013

**Revised:** June 27, 2013

**Published:** August 28, 2013

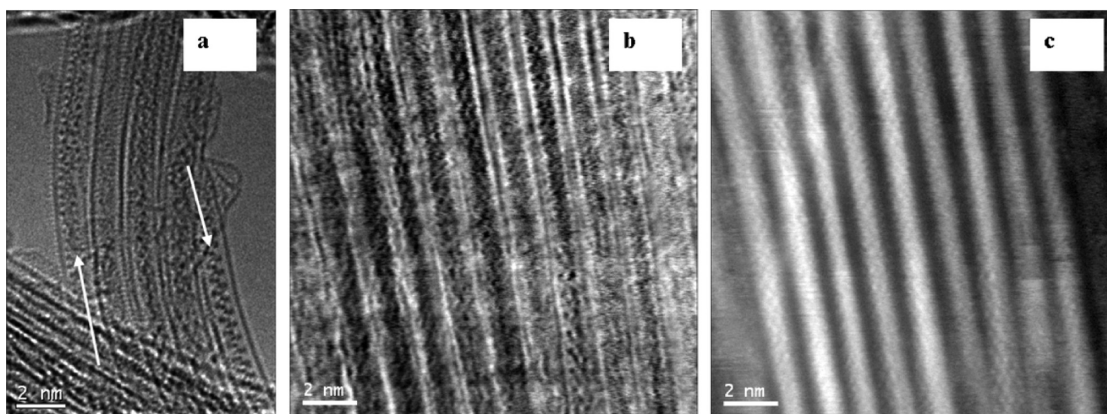


**Figure 1.** Representative HRTEM and STEM data of GeTe nanowires encapsulated within carbon nanotubes, obtained using aberration corrected instruments. (a) HRTEM image of a bundle of SWNTs showing near quantitative filling, containing amorphous (left arrow) and crystalline (right arrow) GeTe filling. Bright-field (b) and dark-field (c) STEM images recorded simultaneously, showing filled SWNT bundles.

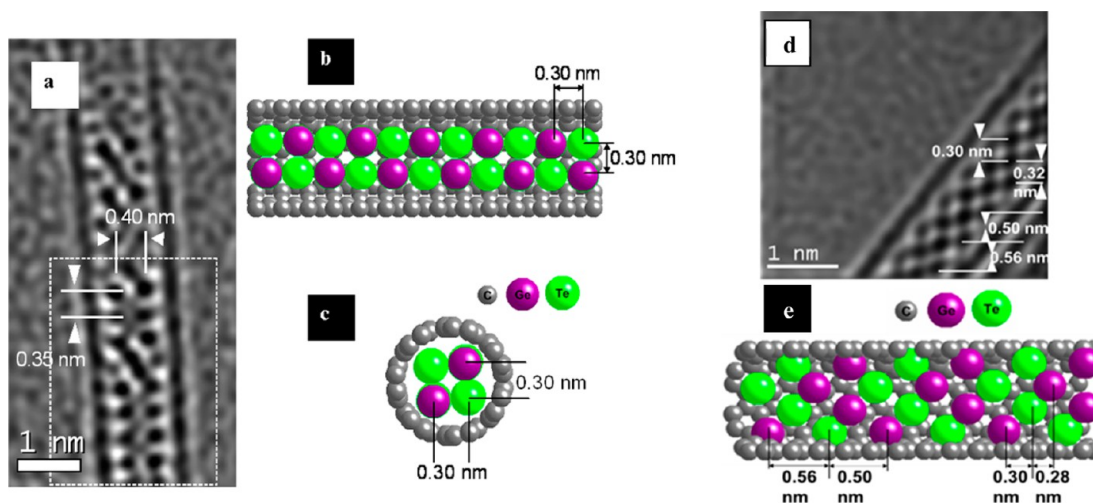


**Figure 2.** Aberration-corrected TEM images and structural models of GeTe encapsulated within nanotubes with different diameters. (a) Aberration-corrected HRTEM image of GeTe rocksalt in a  $2 \times 2$  crystal form within a SWNT, highlighted by the white rectangle, displaying expanded lattice along and across the tube capillary. Structural model of a  $2 \times 2$  GeTe crystal within a carbon nanotube: side-on (b) and end-on (c) representation not incorporating lattice distortions. (d) HRTEM image of a SWNT incorporating GeTe with rhombohedral arrangement, also showing the measured lattice spacing and (e) corresponding structural model.

particle, with the scaling properties only studied down to  $\sim 20$  nm due to technology restrictions in the synthesis of thinner nanowires.

We fabricate nanowires of GeTe, one of the most widely studied phase-change material, within the one-dimensional cavities of SWNTs with diameters of less than 1.4 nm. The central cavities of SWNTs have previously served as a template for engineering one-dimensional structures with novel coordinations and stereochemistries.<sup>21</sup> A wide range of organic,<sup>22–25</sup> as well as inorganic materials<sup>26–28</sup> have been encapsulated within the inner cores of SWNTs with no evidence of a phase-change compound encapsulation reported.

We demonstrate that GeTe can be encapsulated within SWNTs with diameters as low as 1.1 nm that may represent the ultimate size limit in exploring phase-change behavior in these materials at their smallest conceivable scale. Furthermore, we obtain the crystalline form of these systems at this scale and study their fundamental behavior in terms of the atomic structure directly correlated to the electronic properties of the encapsulated material, as derived from scanning tunneling microscopy (STM) and photoelectron spectroscopy.

The methodology used in the preparation of GeTe-filled carbon nanotubes is described in detail in the Supporting Information Section.

High-resolution transmission electron microscopy (HRTEM) data reveal that GeTe has been effectively incorporated within SWNTs (Figure 1a) and energy dispersive X-ray spectroscopy (EDX) analysis (Supporting Information section) indicates the presence of the filling elements Ge and Te within the sample. Additionally, the filled material was examined using scanning transmission electron microscopy (STEM) and representative images are presented in Figure 1b,c.

In the bright-field images (Figure 1b), carbon nanotubes appear with a contrast similar to that in conventional TEM images, whereas in the high-angle annular dark-field images (Z contrast images, Figure 1c), the filling species that have high atomic number  $Z$  compared to the encapsulating C are imaged as discrete, bright wires due to stronger incoherent scattering of the electrons. Within the inner cores of the nanotubes, GeTe forms continuous nanowires with lengths up to a few hundred nanometers. On the basis of a statistical analysis of the TEM

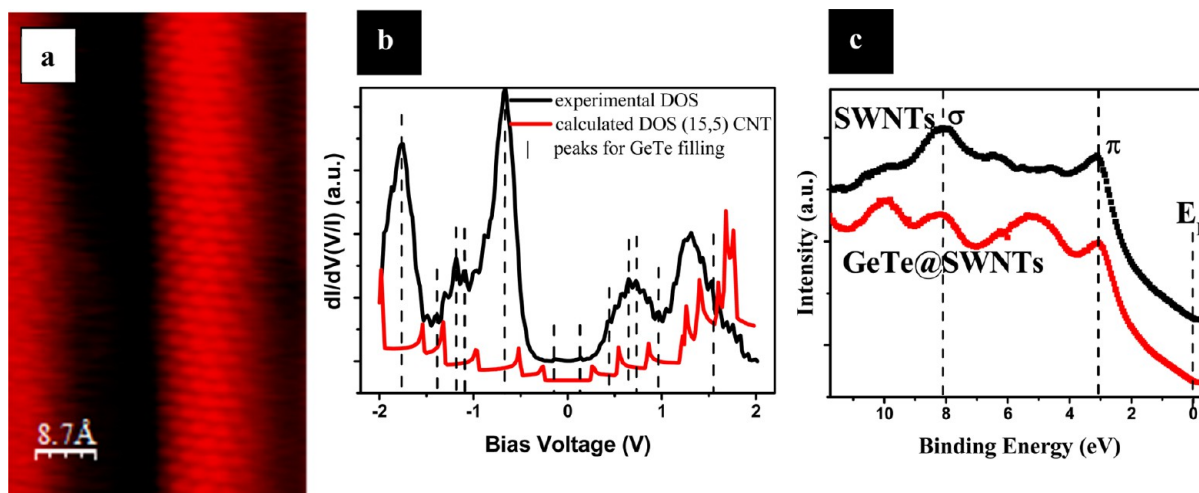


**Figure 3.** Atomic and electronic structure as derived from STM/STS and photoelectron spectroscopy. (a) Atomically resolved image, as revealed by STM, of an individual SWNT of 1.4 nm diameter encapsulating GeTe. (b) Simultaneously recorded scanning tunnelling spectroscopy data on preselected sites along the nanotube, showing a measure of the local density of states (DOS) around the Fermi energy. The calculated DOS for a tube having chiral indices (15, 5) is included in the graph for comparison with the experimental DOS. (c) Ultraviolet photoelectron spectroscopy (UPS) spectra showing the valence band of GeTe-filled SWNTs in comparison to pristine SWNTs, displaying the states associated with the  $\pi$ - and  $\sigma$ -bands of the carbon system below Fermi energy ( $E_F$ ).

data, a filling yield in excess of 80% has been estimated. As indicated by white arrows in Figure 1a, variable crystallization is found, correlated with the nanotubes diameter. For SWNTs with diameters of 1.4 nm, disordered GeTe is obtained, whereas for tubules with diameters of less than or equal to 1.3 nm, crystalline GeTe is observed.

A useful precedent for the diameter-controlled crystallization of amorphous materials was published previously<sup>29</sup> when the formation of amorphous and then glassy eutectic mixtures of  $(\text{KCl})_x(\text{UCl}_4)_y$  was observed within the internal bores of multiwalled carbon nanotubes greater than ca. 1.6–2 nm (amorphous) and less than this diameter crystalline.

Energy minimization conditions within narrow and wide diameters (due to different boundary conditions) will perhaps dictate the end structure so that the crystalline one is more favorable to form in narrow tubes and the disordered structure is favored within the wider nanotubes. However, a rigorous answer as to why a particular structure is favored within a certain range of diameters would only be possible with the aid of density functional theory (DFT) calculations.

Furthermore, for the crystalline case we observe different crystal structures depending on the size of the encapsulating nanotube. A first example is given in Figure 2a that shows the formation of a two-atomic-layer-thick crystal of GeTe within a 1.3 nm diameter SWNT.

As illustrated by the structural model in Figure 2b, the dark spots in the HRTEM image correspond to alternating Ge and Te atoms, maintaining an average periodicity of  $\sim 0.35$  nm along the SWNT axis, consistent with  $d_{-111}$  of bulk cubic GeTe. At room temperature, the bulk GeTe crystal has rhombohedral (distorted rocksalt) structure, which changes to the cubic (rocksalt) structure at high temperatures (above 670 K) by relaxing the slightly distorted angle ( $\sim 88.35^\circ$ ) between the face-centered rhombohedral unit cell axes to the undistorted  $90^\circ$ .<sup>18</sup> GeTe thin films with thicknesses between 1–3 nm are not crystalline in free space, while the rocksalt form of GeTe observed within the encapsulated SWNTs under its forced boundary conditions appears to be stable at room temperature.

The impact of the confinement is also reflected by the modified atomic spacing across the SWNT capillary, observed to increase to 0.4 nm, as highlighted in Figure 2a. Lattice spacing expansion has been reported previously for materials confined within the inner cores of carbon nanotubes.<sup>26–28</sup> This expansion may in part be due to relaxation of the crystal structure in a “too-large” SWNT but could also be due to partial intercalation of the crystal that may also precipitate a different phase forming.

The crystal in Figure 2a appears to be a hybrid between the  $2 \times 2$  GeTe structure as derived from the rocksalt form of this material (the region indicated by the white rectangle in the figure) and the next thickest crystal. Different crystal structures (even for the same material) can be templated by different diameter SWNTs. This is probably because of the effect of the SWNT diameter-regulated crystal growth that can also occur for ordered crystals as described in several theory papers<sup>32</sup> and in the work of Sloan et al.<sup>33</sup> that includes some experimental examples.

Another explanation as to why the top part of the nanotube in Figure 2a looks disordered is that there is a competing effect between the so-called radius-ratio rule (which governs which particular structure type forms for a simple binary halide) and also the confinement effect induced by the small diameter of the encapsulating single-walled carbon nanotube. The top part of the crystal in Figure 2a is probably a slightly expanded  $2 \times 2$  crystal that is in effect accommodating a line-defect of an extra column of atoms in the middle and this is what is causing the disorder at the top of the image.

The possibility of an interface between two crystal growth forms (i.e., between the top and the bottom of the tube) cannot be ruled out either.

As a result of the confinement, we also observe a reduction in the net coordination with respect to the bulk structure, highlighted by the structural model in Figure 2b, and as previously observed on  $2 \times 2$  crystals encapsulated within SWNTs.<sup>28</sup> The rocksalt form of GeTe has octahedral (6:6) coordination in bulk,<sup>30,31</sup> which is reduced to tetrahedral (4:4) coordination upon encapsulation within SWNT capillaries,



possibly responsible for the observed increased spacing of 0.4 nm across the nanotubes.

A further example of GeTe crystal observed within an even narrower SWNT of 1.1 nm diameter is presented in Figure 2d. The GeTe crystal is viewed along its [211] direction and this time it displays the distorted rocksalt (rhombohedral) variant of bulk GeTe. In bulk, the distortion induces the formation of distorted octahedrons with each Te atom surrounded by three Ge at 0.28 nm and three Ge at 0.32 nm.<sup>31</sup> Both the short and long Ge–Te bonds reproduced by the structural model presented in Figure 2e are found in the observed experimental structure by HRTEM, although the values are slightly expanded in each case to 0.30 and 0.32 nm, respectively, possibly as a result of the influence of the nanotube walls.

All of the GeTe nanowires within nanotubes of diameters below 1.3 nm investigated in this study appeared to be crystalline.

To extract information on the electronic behavior of the encapsulated nanowires, scanning tunnelling microscopy has been applied to GeTe-filled carbon nanotubes and the results are depicted in Figure 3a, showing an atomically resolved image of an individual filled SWNT.

Atomically resolved images of SWNTs allow for the determination of the chiral angle,  $\theta$ , which gives the orientation of carbon hexagons with respect to the nanotube axis, and of the diameter,  $d$ , of the tube, both being linked to the structural indices ( $n$ ,  $m$ ) and the electronic structure of the nanotube.<sup>34</sup> The best description for the filled nanotube shown in Figure 3a is given by the chiral indices (15, 5), calculated using  $(1.40 \pm 0.10)$  nm for the diameter and  $(14 \pm 1)^\circ$  for the chiral angle, and thereby expected to be semiconducting in nature. It is interesting to note that the atomic structure of the SWNT presented in Figure 3a does not show the well-known honeycomb structure of carbon hexagons, and instead an outlined structure similar to a Moire pattern, formed by the overlap of the carbon lattice with that of the encased material is observed.<sup>51</sup> The Moire pattern observed here is due to the difference in the lattice constant of GeTe compared to that of the nanotube, which could modify the electronic coupling between the two constituents, causing the changes in conductance seen by the STM. The observed Moire pattern is an indication that in this particular case the GeTe filling has an ordered structure inside the nanotube.

The electronic properties of carbon nanotubes have been shown to be dependent on their atomic structure<sup>34</sup> and this is furthermore reflected by the tunnelling spectra recorded simultaneously with the STM images, using scanning tunnelling spectroscopy (STS). In STS experiments, the current is recorded as a function of the bias applied to the sample to yield the normalized differential conductance,  $(V/I)^*(dI/dV)$ , which is proportional to the electronic local density of states (LDOS).<sup>35</sup> As indicated in Figure 3b, the normalized differential conductance contains sharp peaks, representing the theoretically predicted van Hove singularities (vHs), a clear signature of the LDOS spectra of a 1D system. A detailed analysis of the experimental tunnelling spectra reveals the peaks corresponding to the theoretically predicted van Hove singularities of a (15, 5) tube, but some extra peaks can be identified, highlighted by the vertical lines in Figure 3b. Since the GeTe inner filling is one-dimensional in nature, it is expected to also display van Hove singularities, commensurate with its 1D electronic structure. The theoretically predicted peaks for a carbon nanotube with chirality (15, 5) were

obtained by using density functional theory with local density approximation and made available by Akai and Saito.<sup>36</sup> The peaks associated with the GeTe filling correspond to contributions in the experimental spectra that could not be matched to peaks in the calculated DOS of the (15, 5) nanotube.<sup>38</sup> The poor agreement between the calculated DOS and the experimentally observed data for the filled nanotube could be an indication that the interaction between the nanotube and the filling gives rise to an altered overall electronic structure that, in the low-bias regime, cannot be regarded as the simple overlap of the band structures of the two constituents.

To further probe the interaction between the nanotubes and the filling, ultraviolet photoelectron spectroscopy data has been taken, at an excitation energy of 21.22 eV (He I). These measurements reveal no energy shift of the  $\pi$ -bands of the filled sample with respect to the pristine SWNTs, suggesting the absence of charge transfer between the tubes and the filling, and furthermore showing that the electronic properties of the filled nanotubes and those of the pristine, unfilled nanotubes are not affected by each other's presence. According to a rigid band shift model, the electron transfer from the nanotubes to the filling material would lead to a shift of the Fermi level toward the valence band.<sup>37</sup> The absence of an energy shift means that the electronic structure of the composite can be regarded simply as the overlap of the nanotube states and those of the GeTe filling. It should be noted, however, that UPS is a spatially averaging technique, whereas STM has the ability of probing the local electronic structure at the atomic scale; this could be the reason for the apparent discrepancy between the UPS and the STM observations.

If we assume minimum interaction between the nanotube and the filling, the extra peaks in the experimental DOS can be assigned to GeTe filling, enabling us to estimate a band gap of 0.3 eV associated with the filling, based on the first van Hove singularities at the onset of the valence and conduction band in the tunnelling spectrum. A 0.3 eV value is close to the expected electrical band gap of bulk GeTe. Previous transport studies show that bulk crystalline GeTe is a narrow-band gap semiconductor with an electrical band gap of 0.1–0.2 eV, whereas amorphous GeTe yields an energy gap of 0.8 eV.<sup>39</sup>

A recent *ab initio* molecular dynamics study of GeTe ultrathin films<sup>40</sup> finds that the amorphous film shows a band gap when the film is scaled down to about 3.8 nm (12 atomic layers) but as the film thickness decreases the band gap of the amorphous material disappears (due to overlap of metal-induced gap states near the metal electrodes). The same study<sup>40</sup> shows that GeTe crystalline films in the same size scale show no band gap and the conductance is dominated by the electron transport near the Fermi level.

As previously calculated for the case of carbon nanotubes filled with HgTe,<sup>21</sup> one would expect a larger band gap for GeTe, induced by the extreme confinement within the nanotube than what is currently observed by STM. Bulk HgTe is a semimetal with a band gap of  $-0.3$  eV and DFT determines the bandgap of confined HgTe within the nanotube to be  $+1.3$  eV. It is also known that DFT underestimates the real band gap by ca. 30%, so the band gap value should be even larger.

The assignment of a 0.3 eV band gap for the GeTe filling is done based on the assumption that the overall structure is simply the overlap (the sum) of the two individual band structures, that of the GeTe filling and that of the encasing

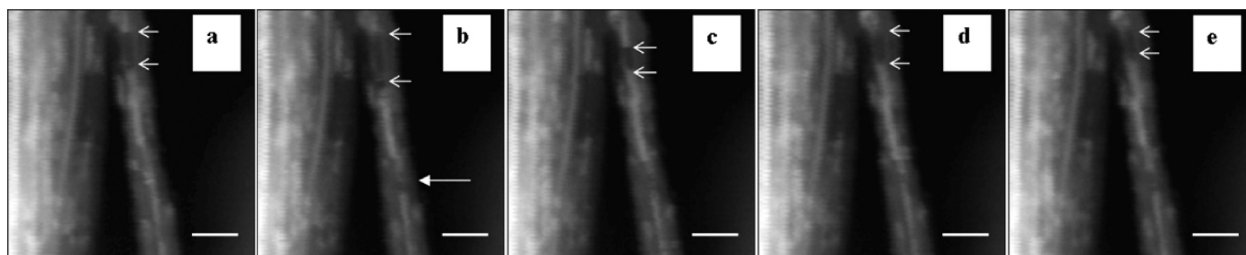


**Figure 4.** Consecutive STEM images displaying a process of void formation and closing in the encapsulated nanowires. (a–e) GeTe filling imaged as bright contrast by STEM-dark-field mode with the white open arrows indicating the change in size of the void created due to material migration under the influence of the electron beam. Arrow in (b) indicates location of a different void previously nonexistent in (a), which seems to almost close in (d) and reopen in (e). Scale bar corresponds to 5 nm in all cases.

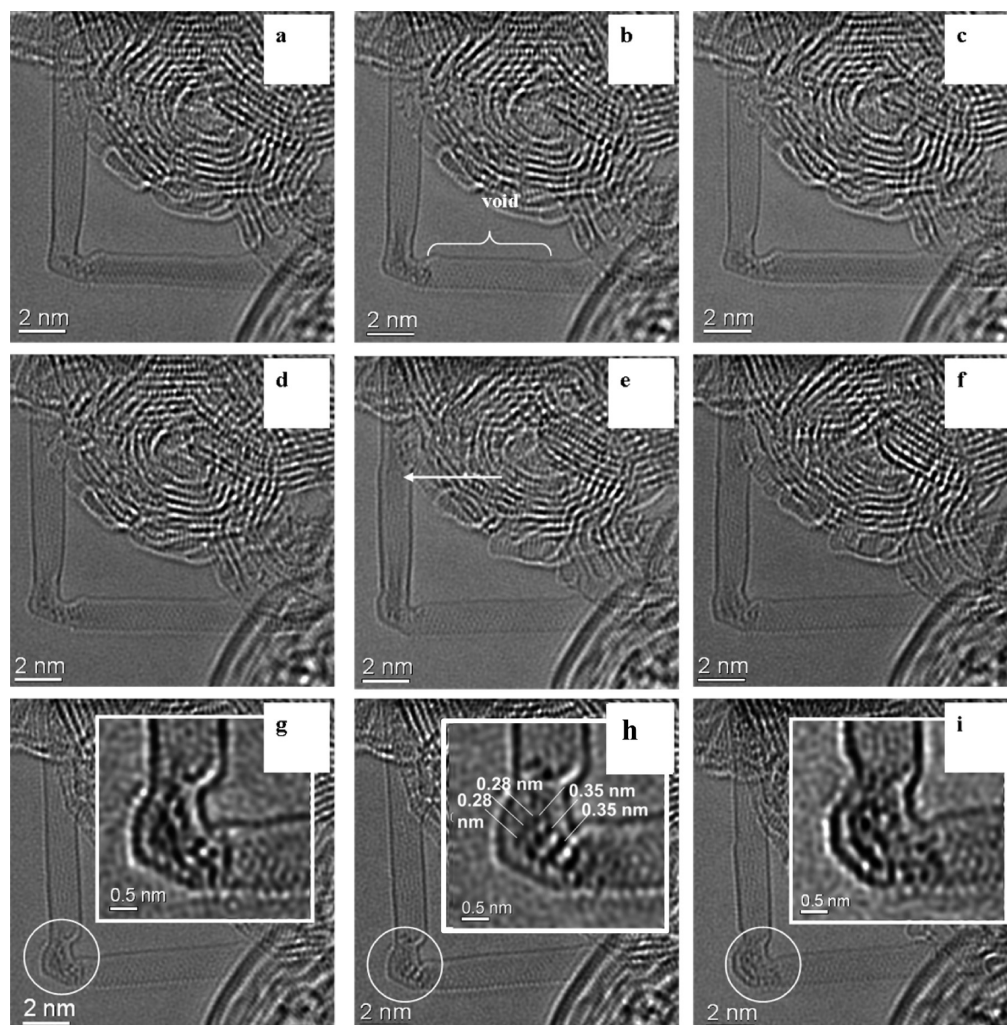


**Figure 5.** HRTEM snapshots selected from a time series showing behavior under electron-beam irradiation of GeTe encapsulated within a SWNT. Consecutive images are presented in b,c and g,h. A video of the entire process is shown in the Supporting Information section. Circled areas in g,h,i, respectively are shown as inset panels.

nanotube. However, this is only valid if the interaction between the nanotube and the filling is not sufficiently strong as to lead to drastic changes in the overall electronic structure of the hybrid system, which is what the STM “sees”. The band gap of the encapsulated materials is an aspect that needs further investigation coupled with DFT calculations of the particular structure presented here for a definite conclusion to be formulated.

It is interesting to observe that Figure 3b shows the Fermi level of the hybrid system inside the band gap, unlike bulk GeTe where the Fermi level is inside the valence band due to defects in the form of Ge vacancies, responsible for the p-type metallic conduction. The current STS observations could possibly indicate that Ge vacancies are no longer the stable defects at such extreme dimensions. On the other hand, charge transfer between the nanotube and the filling might counteract the shift of the Fermi energy to the valence band for the

encapsulated GeTe and show this within the band gap. However, as highlighted in a recent study of encapsulated polyoxometalate ions (n-type dopants) in carbon nanotubes<sup>41</sup> the most rigorous approach to this problem would be a DFT analysis of trial GeTe fillings with the (15,5) SWNT to investigate the electronic structure of the filling.

For applications such as data storage devices, one of the main requirements is that the phase-change compound reversibly changes phase. In the current study, in situ electron-beam irradiation in TEM was used to assess whether the encapsulated GeTe system is structurally affected by the energy of the beam. The highly energetic electrons of a TEM beam can lead to various structural and chemical modifications due to local temperature rise or knock-on damage related effects, depending on the energy of the beam. Physical transformations in materials,<sup>42</sup> conformational changes, and the motion of molecular nanomaterials,<sup>43,44</sup> as well as dynamic processes such as thermal expansion and solid-state diffusion have been examined in real time by TEM.<sup>45</sup> Our investigations take advantage of the aberration-corrected capabilities of both a STEM and TEM, operated at low acceleration voltages of 80 kV, below the knock-on structural damage of the sp<sup>2</sup> carbon bonding. This is shown to induce reactions in the encapsulated material, without producing significant damage to the nanotube host.<sup>46</sup>

A sequence of five experimental STEM images of GeTe encapsulated within a SWNT, obtained at intervals over a period of 100 s, is shown in Figure 4a–e.

Under the influence of the electron beam, the filling is observed to move back and forth within the nanotube, sometimes creating mobile voids that change size, open, and close, as illustrated by the image sequence in the panels below.

Not all encapsulated nanowires show void formation, as in some cases the filling appears to be stable under the electron beam, suggesting the presence of defects on the surface of the nanotubes as a possible cause for the observed motion of the encapsulated material.

The flow of the filling, sometimes involving the back and forth oscillations of the entire nanowire, is also observed under TEM, which allowed us to investigate the filling within the nanowire in considerable detail and to assess whether the movement involves structural rearrangement upon electron-beam irradiation. The effect of local heating induced by focusing the electron beam under simultaneous TEM observation is illustrated in Figure 5.

Figure 5 shows a series of representative HRTEM images of an “L” shaped SWNT host containing GeTe filling, selected from a video recorded over a period of 20 min with 4 frames per second at exposure time of 0.2 s. (For the entire movie see the Supporting Information section.) The difference in contrast inside the two orthogonal segments of the nanotube in the initial image (Figure 5a) highlights the presence of the filling material.

The fast Fourier transform (FFT) of the filled segment (Figure S1 in Supporting Information section) shows reflections associated with the encapsulating nanotube and the absence of structure associated with the filling material, suggesting that the encapsulated material has undergone a phase transformation to an amorphous state, driven by atoms rearrangement under the influence of the electron-beam.

The movement of the filling material along the inner walls of the encapsulating nanotube is constantly observed by TEM, throughout the entire duration of the e-beam-irradiation

process (Figure 5b–e). After approximately 1.5 min irradiation time, the filling starts to show the same oscillatory movement observed in the STEM of void formation and closing. The filling separates into two sections (Figure 5b), which rejoin in the next consecutive frame (Figure 5c), taken at 4 s intervals. In Figure 5d,e, the molten core starts to move upward and a portion of the filling, indicated by the white arrow, becomes visible at the top end of the vertical segment of the nanotube.

Similar movement phenomena have been previously observed in other core–shell heterostructured systems, such as Sn-filled In(OH)<sub>3</sub> nanotubes,<sup>47</sup> Sn-filled ZnS nanotubes,<sup>48</sup> or C<sub>60</sub> molecules encapsulated within SWNTs.<sup>44</sup> A possible explanation could be that the movement is due to charge fluctuation effects, as previously observed by Iijima et al.<sup>49</sup> for the case of 2 nm diameter Au nanoparticles subject to intense electron-beam irradiation with the rate of movement increased by a decrease in the contact area of the particle with the substrate. In our case, the movement is also intensified for nanotubes lying over the voids of the holey carbon grid substrate, where the heat dissipation occurs only through the tube itself and therefore it is expected to have a higher local temperature when irradiated.

Loss of filling material becomes evident in panel f of Figure 5, where no filling is observed in either of the two orthogonal branches of the nanotube, being only present at the bend region, indicated by the white circle, where it remains for the last 10 min of the electron-beam irradiation experiment. Loss of material could be due to solid-state diffusion along the nanotube and transport through one or both open ends of the host nanotube. It is possible that the encapsulated nanowire is only stable within the forced boundary conditions of the carbon nanotube shell. The motion observed within the carbon nanotube could be therefore due to solid-state diffusion caused by atomic rearrangement from an unstable phase of the GeTe filling, when the electron beam slightly damages the encapsulating nanotube, to a more stable morphology.

At the final stages of the irradiation experiment, the remaining material observed at the bend can be regarded as an irregular-shaped nanoparticle with a varying size of approximately 0.5 to 0.75 nm wide and between 1 and 1.5 nm in length. Structural modifications are constantly observed for the encapsulated GeTe, and both disordered, as well as ordered structures are found, seemingly correlated with the change in shape of the confining space, as illustrated in Figure 5g–i. Amorphous phases of GeTe are evidenced in Figure 5g and inset panel, and the visualization of the first GeTe structural ordering of the series is given in the next consecutive image (Figure 5h), where lattice planes of approx 0.28 nm across and 0.35 nm along the capillary, marked on the inset panel, are visible. These values are very close to the values estimated for the 2 × 2 GeTe rocksalt crystal encapsulated within a nanotube of 1.3 nm diameter presented in Figure 2a with the difference due to the difference in size of the confining space that appears to favor an incipient 3 × 3 GeTe rocksalt crystal (Figure 5h). The crystal seeds disappear later to form again an amorphous structure, as indicated in Figure 5i. It is important to note that even though transient the encapsulated GeTe shows the ability to change phase and crystallize at dimensions less than 2 nm, contrary to previous studies, and extending the size limit to explore associated scaling properties for phase-change memory devices. The conditions of our current experimental study do not enable a clear quantification of the phase-change process in terms of the amorphous-to-



crystal transition temperature or melting point associated with a size of 1 nm, since the specimen is subject to continuous electron-beam irradiation and additional factors, such as knock-on related effects, causing constant changes in the nanotube's shape, which influence the outcome.

As highlighted in Figure 5 and throughout the entire duration of the electron irradiation experiment, we observe contraction behavior of the encapsulating nanotube caused by knocking carbon atoms out, followed by atomic lattice reconstruction. The nanotube preserves the overall L shape, however small variations in diameter and constant changes in its shape at the bend region are observed even at 80 kV acceleration voltage. Although the knock-on structural threshold damage for carbon nanotube systems is known to be approximately 86 keV,<sup>50</sup> the variations observed could be due to strain associated with the bend or possibly due to growth defects existent in the nanotube's atomic network (such as pentagon–heptagon pairs) that render the “L” shape. Previous studies showed that the deformation of nanotubes filled with Fe<sub>3</sub>C under electron irradiation caused extrusion of the filling material under the pressures prevailing inside nanotubes.<sup>42</sup> The pressure inside a single shell was estimated at 20 GPa for a (10, 10) carbon nanotube (diameter 1.35 nm, similar to our investigated diameter range) with a double-vacancy concentration of 0.06. Similarly, the structural changes we observe in the current study could be due to pressure-induced compressive forces associated with changes in shape of the nanotube and of the bent region.

It should be pointed out that the images in Figure 5 are time-resolved images, that is, they are showing the phase change behavior as a result of extended beam irradiation. This is in contrast to images shown in Figure 2 that are “single shot” images, presumably if these were held in the beam for longer, the crystal structure would degrade.

In conclusion, a phase change material with 1D structure has been obtained by filling the inner cores of nanometer diameter carbon nanotubes with GeTe, and the material was characterized. This methodology developed offers the advantage of a very small integrated structure in addition to a uniform morphology of the encased structures unlike catalyst-assisted vapor–liquid–solid synthesis methods that result in mixed morphologies (straight, helical, etc. nanowires). The catalyst-produced structures often contain other impurities and always exhibit an oxide layer on the surface of the nanowire. The protective shell of the carbon nanotube prevents oxidation of the encapsulated nanowire and helps maintain the nanowire's chemical composition integrity due to the inertness of the surrounding nanotube.

The reduced dimensionality of the encapsulated GeTe presents the advantage of a lower melting point compared to that of the bulk material, and therefore is advantageous for lowering writing/erasing currents required for phase switching, should these structures be possible to integrate into memory devices. Our results further demonstrate that GeTe crystallizes in the rocksalt form within nanotube capillaries of diameters as low as 1.3 nm, below the predicted 2 nm limit for crystallization at this scale. In-situ TEM analysis shows rapid transformations of the encapsulated GeTe structure under the influence of electron-beam irradiation. Amorphous to crystalline changes are evidenced at this scale, fulfilling an important prerequisite of a phase-change material, with reversible switching between the disordered and ordered phases.

The current study shows evidence for the smallest phase-change material synthesized to date and extends the size limit to explore the suitability of this material for nonvolatile memory devices.

## ■ ASSOCIATED CONTENT

### Supporting Information

This section contains experimental details consistent with the main content, as well as a video showing the encapsulated GeTe's behavior under electron beam irradiation. This material is available free of charge via the Internet at <http://pubs.acs.org>.

## ■ AUTHOR INFORMATION

### Corresponding Author

\*E-mail: [cristina.giusca@npl.co.uk](mailto:cristina.giusca@npl.co.uk).

### Present Addresses

<sup>#</sup>(C.E.G.) National Physical Laboratory, Hampton Road, Teddington, TW11 0LW, United Kingdom.

<sup>∇</sup>(F.B.) Speziallabor Triebenbergl, Institut für Strukturphysik, Technische Universität Dresden, 01062 Dresden, Germany.

<sup>○</sup>(H.S.) Faculty of Physics, University of Vienna, Strudlhofgasse 4, 1090 Vienna, Austria.

### Notes

The authors declare no competing financial interest.

## ■ ACKNOWLEDGMENTS

The work was supported by EPSRC Grants EP/F052901/1 and GR/S72320/01

## ■ REFERENCES

- (1) Ovshinsky, S. R. Reversible electrical switching phenomena in disordered structures. *Phys. Rev. Lett.* **1968**, *21*, 1450–1453.
- (2) Wuttig, M.; Yamada, N. Phase-change materials for rewritable data storage. *Nat. Mater.* **2007**, *6*, 824–832.
- (3) Raoux, S. Phase change materials. *Ann. Rev. Mat. Res.* **2009**, *39*, 25–48.
- (4) Raoux, S.; Welnic, W.; Ielmini, D. Phase Change Materials and Their Application to Nonvolatile Memories. *Chem. Rev.* **2010**, *110*, 240–267.
- (5) Yu, D.; Brittan, S.; Lee, J. S.; Falk, A. L.; Park, H. Minimum Voltage for Threshold Switching in Nanoscale Phase-Change Memory. *Nano Lett.* **2008**, *8*, 3429–3433.
- (6) Raoux, S.; Burr, G. W.; Breitwisch, M. J.; Rettner, C. T.; Chen, Y.-C. Phase-change random access memory: A scalable technology. *IBM J. Res. Dev.* **2008**, *52* (4/5 July/September), 465.
- (7) Siegrist, T.; Jost, P.; Volker, H.; Woda, M.; Merkelbach, P.; Schlockermann, C.; Wuttig, M. Disorder-induced localization in crystalline phase-change materials. *Nat. Mat.* **2011**, *10*, 202–208.
- (8) Xiaoqian, W.; Luping, S.; Chong, C. T.; Rong, Z.; Koon, L. H. Thickness dependent nano-crystallization in Ge<sub>2</sub>Sb<sub>2</sub>Te<sub>5</sub> films and its effect on devices. *Jpn. J. Appl. Phys.* **2007**, *46*, 2211–2214.
- (9) Rueckes, T.; Kim, K.; Joselevich, E.; Tseng, G. Y.; Cheung, C.; Lieber, C. M. Carbon Nanotube-based nonvolatile random access memory for molecular computing. *Science* **2000**, *289*, 94–97.
- (10) Xiong, F.; Liao, A. D.; Estrada, D.; Pop, E. Low-Power Switching of Phase-Change Materials with Carbon Nanotube Electrodes. *Science* **2011**, *332*, 568–570.
- (11) Xiong, F.; Bae, M.-H.; Dai, Y.; Liao, A. D.; Behnam, A.; et al. Self-Aligned Nanotube–Nanowire Phase Change Memory. *Nano Lett.* **2013**, *13*, 464.
- (12) Milliron, D. J.; Raoux, S.; Shelby, R.; Jordan-Sweet, J. Solution-phase deposition and nanopatterning of GeSbSe phase-change materials. *Nat. Mater.* **2007**, *6*, 352–356.

- (13) Chung, H. B.; Shin, K.; Lee, J. M. Phase-change characteristics of chalcogenide  $\text{Ge}_1\text{Se}_1\text{Te}_2$  thin films for use in nonvolatile memories. *J. Vac. Sci. Technol. A* **2007**, *25*, 48–53.
- (14) Kolobov, A. V.; et al. Understanding the phase-change mechanism of rewritable optical media. *Nat. Mater.* **2004**, *3*, 703–708, DOI: 10.1038/nmat1215.
- (15) Raoux, S.; et al. Direct observation of amorphous to crystalline phase transitions in nanoparticle arrays of phase change materials. *J. Appl. Phys.* **2007**, *102*, 8.
- (16) Lee, S. H.; Jung, Y.; Agarwal, R. Highly scalable non-volatile and ultra-low power phase-change nanowire memory. *Nature Nanotechnol.* **2007**, *2*, 626–630.
- (17) Meister, S.; et al. Synthesis and Characterization of Phase-Change Nanowires. *Nano Lett.* **2006**, *6*, 1514–1517.
- (18) Sun, X. H.; Yu, B.; Ng, G.; Meyyappan, M. One-Dimensional Phase-Change Nanostructure: Germanium Telluride Nanowire. *J. Phys. Chem. C* **2007**, *111*, 2421–2425.
- (19) Wright, C. D.; Armand, M.; Aziz, M. M. Terabit-per-square-inch data storage using phase-change media and scanning electrical nanoprobes. *IEEE Trans. Nanotechnol.* **2006**, *5*, 50–61.
- (20) Raoux, S.; Jordan-Sweet, J. L.; Kellock, A. J. Crystallization properties of ultrathin phase change films. *J. Appl. Phys.* **2008**, *103*, 7.
- (21) Carter, R.; et al. Correlation of structural and electronic properties in a new low-dimensional form of mercury telluride. *Phys. Rev. Lett.* **2006**, *96*, 215501.
- (22) Li, L. J.; Khlobystov, A. N.; Wiltshire, J. G.; Briggs, G. A. D.; Nicholas, R. J. Diameter-selective encapsulation of metallocenes in single-walled carbon nanotubes. *Nat. Mater.* **2005**, *4*, 481–485.
- (23) Pichler, T. Molecular nanostructures: Carbon ahead. *Nat. Mater.* **2007**, *6*, 332.
- (24) Shiozawa, H.; et al. A catalytic reaction inside a single-walled carbon nanotube. *Adv. Mater.* **2008**, *20*, 1443–1449.
- (25) Hornbaker, D. J.; et al. Mapping the one-dimensional electronic states of nanotube peapod structures. *Science* **2002**, *295*, 828–831.
- (26) Sloan, J.; Kirkland, A. I.; Hutchison, J. L.; Green, M. L. H. Aspects of crystal growth within carbon nanotubes. *C. R. Phys.* **2003**, *4*, 1063–1074.
- (27) Meyer, R. R.; et al. Discrete atom imaging of one-dimensional crystals formed within single-walled carbon nanotubes. *Science* **2000**, *289*, 1324–1326.
- (28) Sloan, J.; Kirkland, A. I.; Hutchison, J. L.; Green, M. L. H. Integral atomic layer architectures of 1D crystals inserted into single walled carbon nanotubes. *Chem. Commun.* **2002**, 1319–1332.
- (29) Sloan, J.; Cook, J.; Chu, A.; Zweifka-Sibley, M.; Green, M. L. H.; Hutchison, J. L. Selective Deposition of  $\text{UCl}_4$  and  $(\text{KCl})_x(\text{UCl}_4)_y$  inside Carbon Nanotubes Using Eutectic and Noneutectic Mixtures of  $\text{UCl}_4$  with KCl. *Solid State Chem.* **1998**, *140*, 83–90.
- (30) Welnic, W.; Wuttig, M.; Botti, S.; Reining, L. Local atomic order and optical properties in amorphous and laser-crystallized GeTe. *C. R. Phys.* **2009**, *10*, 514–527.
- (31) Da Silva, J. L. F.; Walsh, A.; Lee, H. L. Insights into the structure of the stable and metastable  $(\text{GeTe})_m(\text{Sb}_2\text{Te}_3)_n$  compounds. *Phys. Rev. B* **2008**, *78*, 224111.
- (32) Wilson, M. Structure and phase stability of novel twisted crystal structures in carbon nanotubes. *Chem. Phys. Lett.* **2002**, *366*, 504.
- (33) Sloan, J.; Kirkland, A. I.; Hutchison, J. L.; Green, M. L. H. Aspects of crystal growth within carbon nanotubes. *C. R. Phys.* **2003**, *4*, 1063.
- (34) Odom, T. W.; Huang, J. L.; Kim, P.; Lieber, C. M. Atomic structure and electronic properties of single-walled carbon nanotubes. *Nature* **1998**, *391*, 62–64.
- (35) Stroschio, J. A.; Feenstra, R. M.; Fein, A. P. Electronic-structure of the  $\text{Si}(111)2 \times 1$  surface by scanning-tunneling microscopy. *Phys. Rev. Lett.* **1986**, *57*, 2579–2582.
- (36) Akai, Y.; Saito, S. Electronic structure, energetics and geometric structure of carbon nanotubes: A density-functional study. *Physica E* **2005**, *29*, 555.
- (37) Rauf, H.; et al. Influence of the C-60 filling on the nature of the metallic ground state in intercalated peapods. *Phys. Rev. B* **2005**, *72*, 245411.
- (38) Giusca, C. E.; Tison, Y.; Stolojan, V.; Borowiak-Palen, E.; Silva, S. R. P. Inner-tube chirality determination for double-walled carbon nanotubes by scanning tunneling microscopy. *Nano Lett.* **2007**, *7*, 1232–1239.
- (39) Bahl, S. K.; Chopra, K. L. Amorphous versus Crystalline GeTe Films. III. Electrical Properties and Band Structure. *J. Appl. Phys.* **1970**, *41* (5), 2196.
- (40) Liu, J.; Anantram, M. P. Low-bias electron transport properties of germanium telluride ultrathin films. *J. Appl. Phys.* **2013**, *113*, 063711.
- (41) Bichoutskaia, E.; Liu, Z.; Kuganathan, N.; Faulques, E.; Suenaga, K.; Shannond, I. J.; Sloan, J. High-precision imaging of an encapsulated Lindqvist ion and correlation of its structure and symmetry with quantum chemical calculations. *Nanoscale* **2012**, *4*, 1190.
- (42) Sun, L.; et al. Carbon nanotubes as high-pressure cylinders and nanoextruders. *Science* **2006**, *312*, 1199–1202.
- (43) Sloan, J.; et al. Direct Imaging of the Structure, Relaxation, and Sterically Constrained Motion of Encapsulated Tungsten Polyoxometalate Lindqvist Ions within Carbon Nanotubes. *ACS Nano* **2008**, *2*, 966–976.
- (44) Warner, J. H.; et al. Capturing the Motion of Molecular Nanomaterials Encapsulated within Carbon Nanotubes with Ultrahigh Temporal Resolution. *ACS Nano* **2009**, *3*, 3037–3044.
- (45) Holmberg, V. C.; Panthani, M. G.; Korgel, B. A. Phase transitions, melting dynamics, and solid-state diffusion in a nano test tube. *Science* **2009**, *326*, 405–407.
- (46) Warner, J. H.; et al. One-dimensional confined motion of single metal atoms inside double-walled carbon nanotubes. *Phys. Rev. Lett.* **2009**, *102*, 4.
- (47) Fang, Y.; Wen, X.; Yang, S. Hollow and tin-filled nanotubes of single-crystalline  $\text{In}(\text{OH})_3$  grown by a solution-liquid-solid-solid route. *Angew. Chem., Int. Ed.* **2006**, *45*, 4655–4658.
- (48) Hu, J. Q.; Bando, Y.; Zhan, J. H.; Golberg, D. Sn-filled single-crystalline wurtzite-type ZnS nanotubes. *Angew. Chem., Int. Ed.* **2004**, *43*, 4606–4609.
- (49) Iijima, S.; Ichihashi, T. Structural instability of ultrafine particles of metals. *Phys. Rev. Lett.* **1986**, *56*, 616–619.
- (50) Smith, B. W.; Luzzi, D. E. Electron irradiation effects in single wall carbon nanotubes. *J. Appl. Phys.* **2001**, *90*, 3509.
- (51) Tison, Y.; Giusca, C. E.; Sloan, J.; Silva, S. R. P. Registry-Induced Electronic Superstructure in Double-Walled Carbon Nanotubes, Associated with the Interaction between Two Graphene-Like Monolayers. *ACS Nano* **2008**, *2*, 2113.